



Non-Polluting Composites Repair
and Remanufacturing
for Military Applications:
Induction-Based Repair
of Integral Armor

by Bruce K. Fink, Steven H. McKnight,
Shridhar Yarlagadda, and John W. Gillespie Jr.

ARL-TR-2121

November 1999

19991126 089

Approved for public release; distribution is unlimited.

The findings in this report are not to be construed as an official Department of the Army position unless so designated by other authorized documents.

Citation of manufacturer's or trade names does not constitute an official endorsement or approval of the use thereof.

Destroy this report when it is no longer needed. Do not return it to the originator.

Army Research Laboratory

Aberdeen Proving Ground, MD 21005-5069

ARL-TR-2121

November 1999

Non-Polluting Composites Repair and Remanufacturing for Military Applications: Induction-Based Repair of Integral Armor

Bruce K. Fink and Steven H. McKnight
Weapons and Materials Research Directorate, ARL

Shridhar Yarlagadda and John W. Gillespie Jr.
University of Delaware

Abstract

Polymer-matrix composite material and structural adhesive repair and manufacturing have significant environmental costs. These costs have recently been documented based on current and anticipated future Department of Defense (DOD) use of these materials. The principal issues for reducing the environmental impact and its associated cost are (1) reduction in hazardous waste by eliminating shelf-life limitations, (2) reduction in nitrogen oxides (NO_x) by replacing global heating of the part with localized heating, (3) reduction in volatile organic compound (VOC) emissions by accelerated curing and containment, and (4) reduction in hazardous waste by minimizing production debris through processing step management. Induction-based adhesive curing is a potential replacement for current repair and manufacturing methods to resolve the principal issues. The current work establishes that induction heating using conductive mesh susceptors can be used to rapidly cure thermosetting adhesives under a VOC-reducing vacuum condition. It is also established that the presence of these susceptor materials, although not optimized, does not adversely affect the mechanical performance of the bondline when considering the low scatter in lap shear strength. The feasibility of induction-based repair using metallic screen susceptors and the applicability of induction heating to multilayer single-step bonding wherein heat generation is limited to localized bondline regions allowing optimization of repair processes are demonstrated.

Acknowledgments

This research was supported in part by the U.S. Department of Defense (DOD), through the Strategic Environmental Research and Development Program (SERDP). The authors gratefully acknowledge the assistance of Diane Kukich (Editorial Coordinator at the University of Delaware Center for Composite Materials) in editing and publishing this report. The authors also gratefully acknowledge the collaborative research efforts of Dr. Tong Earn Tay (National University of Singapore), Sean M. Wells (University of Delaware), and Roman Berger (University of Aachen).

INTENTIONALLY LEFT BLANK.

Table of Contents

| | <u>Page</u> |
|---|-------------|
| Acknowledgments | iii |
| List of Figures | vii |
| List of Tables | ix |
| 1. Introduction | 1 |
| 2. Background on Induction-Based Repair | 3 |
| 2.1 Conductive Mesh Susceptors..... | 3 |
| 2.2 Magnetic Particle Susceptors..... | 4 |
| 2.3 Carbon-Fiber Composites..... | 4 |
| 2.4 Induction Heating System..... | 6 |
| 3. Induction-Based Accelerated Cure of Adhesives | 8 |
| 3.1 Characterization of Cure Kinetics..... | 9 |
| 3.2 Performance Comparison of Adhesive Systems..... | 16 |
| 4. Induction-Based Repair of Integral Armor | 18 |
| 4.1 Susceptor and Coil Design..... | 19 |
| 4.2 Coil Motion Studies..... | 19 |
| 4.3 Composite Armor Subsystem Bonding..... | 21 |
| 4.4 One-Step Multilayer Composite Bonding..... | 22 |
| 5. Conclusions | 27 |
| 6. References | 29 |
| Distribution List | 31 |
| Report Documentation Page | 41 |

INTENTIONALLY LEFT BLANK.

List of Figures

| <u>Figure</u> | <u>Page</u> |
|--|-------------|
| 1. Induction Apparatus for Repair and Processing of Composite Parts | 2 |
| 2. Eddy Currents Induced in a Conductive Material | 3 |
| 3. Model of Magnetic Domains During Hysteresis Loss | 5 |
| 4. Hysteresis Loops in Ferromagnetic Materials..... | 5 |
| 5. Schematic of Heating Mechanism in Carbon-Fiber-Based Composites [7] | 6 |
| 6. Open-Loop Response of Induction Heating System | 7 |
| 7. Induction Heater Response With Manual Control | 7 |
| 8. Induction System Response With PID Feedback Control | 8 |
| 9. Comparison of Kinetics Model Cure Times to Experimental Cure Times for Varying Degrees of Cure | 12 |
| 10. SLS Specimen Fabricated Setup With Copper Wire Mesh Susceptors and Hysol EA9394 Adhesive | 15 |
| 11. Temperature Profile of SLS Specimens Demonstrating Uniformity of Heating in Process Window Enabled by Induction Heating for Repair..... | 15 |
| 12. Plot Showing $\pm 3\sigma$ Performance of SLS Specimens..... | 17 |
| 13. Section of Typical Multilayered Multifunctional Composite Armor Panel..... | 18 |
| 14. Temperature Profile of Ceramic Tile/Steel Mesh | 20 |
| 15. Comparison of Temperature Profiles After 20 min of Heating (a) Without Coil Motion and (b) With Coil Motion | 20 |
| 16. Temperatures of Lines LI01 in Figure 15 | 21 |
| 17. Surface Temperature Variation During Bonding of Ceramic Tile to 7/16-in-Thick Glass/Epoxy Composite With Coil Motion | 23 |

| <u>Figure</u> | <u>Page</u> |
|---|-------------|
| 18. Schematic of Lay-Up Sequence for One-Step Induction Repair of Composite Armor Panel..... | 24 |
| 19. Surface Temperature Profile for Single-Step Bonding with Coil Motion | 25 |
| 20. Surface Temperature Variation at Two Different Locations | 25 |
| 21. Spot Locations for IR Camera Temperature Measurement | 26 |
| 22. Time/Temperature Response During One-Step Induction Bonding as Measured by IR Camera..... | 26 |
| 23. Single-Step Bonded Multilayer Composite Specimen..... | 27 |

List of Tables

| <u>Table</u> | | <u>Page</u> |
|--------------|---|-------------|
| 1. | Cure Kinetics Model Parameters for Hysol EA9394 | 11 |
| 2. | Lap Shear Data for Hysol EA9394 | 13 |
| 3. | Temperature Measurements at the Surface and Bondline..... | 23 |

INTENTIONALLY LEFT BLANK.

1. Introduction

The search for cost-effective environmentally friendly manufacturing methods has led to the study of induction heating for bonding and processing of composites. Electromagnetic cure methods involve using induction or electrical resistance heating focused directly at the material to be cured. Induction heating occurs when a current-carrying body, or coil, is placed near another conductor, the susceptor material. The magnetic field caused by the current in the coil induces a current in the susceptor. This induced current causes the susceptor to heat due to Joule heating and, in the case of a ferromagnetic material, due to hysteresis losses. Carbon-fiber reinforcement in composite materials can function as the susceptor. For other material systems, the susceptor is a metallic mesh or magnetic particles. Energy can be introduced into the precise region to be cured both in the plane of the structure and at the specific depth required.

Advantages of induction include reduction of volatile organic compounds (VOCs) and nitrous oxide (NO_x) emissions by processing out of the autoclave and processing a much smaller volume. Eliminating processing steps reduces hazardous waste, and energy consumption is also reduced. Other advantages of induction include internal non-contact heating; the possibility of a moving heat source (the coil) to heat large areas; high efficiency; control of the heat generation by coil design or by susceptor design; and powerful, portable, and easy-to-operate units.

Supplying the energy needed for curing thermoset resins and adhesives or for thermoplastic bonding is a critical concern in field repair applications, and induction heating is an ideal choice. Research to date [1-6] has demonstrated that this method shows great promise for rapid repair and processing of composite parts. The induction setup is shown in Figure 1.

Induction heating has many advantages over competing techniques, such as radiant or convection heating and laser technologies. Some of the main advantages are as follows.

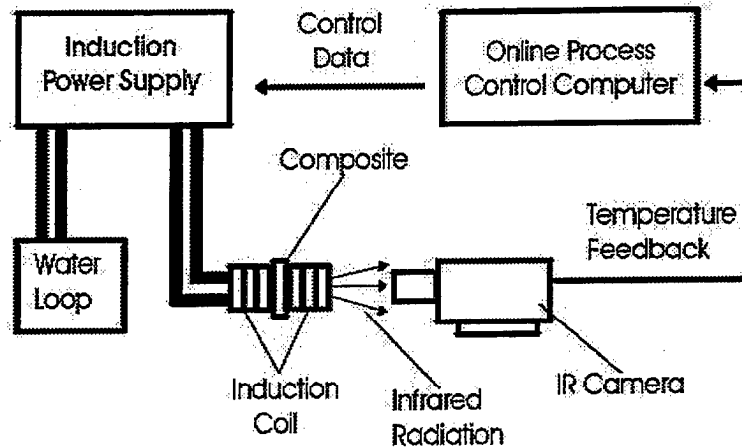


Figure 1. Induction Apparatus for Repair and Processing of Composite Parts.

- **Environmentally sound**—Clean non-polluting process exhibits reduced VOC emissions.
- **Accurate temperature control**—Direct control of temperature is possible through continuous power control.
- **Localized volumetric heating**—Uniform heating through the thickness of the bondline reduces warpage and residual stresses.
- **Improved quality**—Contact-free process induces heat in the product without contact, thus reducing the rate of rejected parts.
- **Minimized distortion**—Site-specific process delivers heat exactly where it is needed and as rapidly as needed, so other locations on the part are not exposed to heat flux.
- **Energy-efficient process**—Up to 80% of the expended energy is converted into useful heat to save costs.
- **Maximized productivity**—Instantaneous heat allows for increased production rates.

The current Strategic Environmental Research and Development Program (SERDP) effort seeks to exploit these advantages and develop induction-based processing and repair technologies for composites used in DOD applications.

2. Background on Induction-Based Repair

Induction heating occurs when materials are subjected to a high-frequency magnetic field. The two primary heating mechanisms are eddy-current-based heating and magnetic hysteresis-based heating. For composites, both mechanisms are embodied in three classes of susceptors or heating elements: conductive mesh/adhesive or resin systems, magnetic particle-based resin or adhesive systems, and carbon-fiber-reinforced composites. Carbon-fiber-based composites are treated as a separate class because the heating mechanism is somewhat different, even though it is the conductivity of the fibers that causes heating. Each class is discussed in the following sections.

2.1 Conductive Mesh Susceptors. The change of magnetic flux induces eddy currents in the conductive mesh, and heating occurs primarily by Joule heating (Figure 2). Eddy currents are magnetically induced body currents in the material that flow primarily in peripheral loops perpendicular to the field so as to create flux fields, which oppose the magnetic field. As the frequency of the applied magnetic field increases, eddy currents are increasingly generated in the outer layers of the conductor (skin effect).

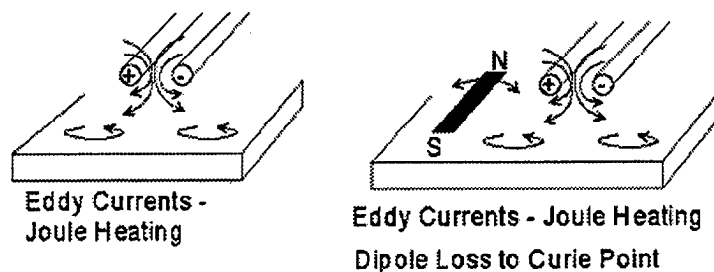


Figure 2. Eddy Currents Induced in a Conductive Material.

In our research for SERDP, metal wire meshes, typically made from copper, aluminum, or stainless steel, are impregnated with an appropriate adhesive or resin and placed at the bondline. The magnetic field is applied to generate heat and cure the adhesive or resin system. The mesh wires may also be surface-treated to improve adhesion between the mesh wires and the resin or adhesive system.

This program is taking advantage of enabling technologies co-developed by the U.S. Army Research Laboratory (ARL) and the University of Delaware Center for Composite Materials (UD-CCM) in which the metal mesh susceptors are specially designed for optimized in-plane heating [1-6].

2.2 Magnetic Particle Susceptors. Induction heating can also occur due to hysteresis losses. Hysteresis losses occur in ferromagnetic materials such as iron and nickel. Heat generation is caused by friction between magnetic domains when the material is magnetized first in one direction and then in the other. The domains may be regarded as small magnets that turn around with each reversal of direction of the magnetic field (Figure 3). Work (energy) is required to turn them around. The rate of expenditure of energy (power) increases with an increased rate of reversal (frequency). The energy required to turn the internal magnet around once is proportional to the area enclosed by the hysteresis loop (Figure 4) of the material. The hysteresis loop relates induced magnetic flux density to the applied magnetizing force. Hysteresis heating may or may not be the main heating effect, depending on the part geometry.

In current research, magnetic fields are applied to magnetic-particle-loaded resin systems. Specialized adhesive systems are being formulated with magnetic particle content of up to 20-30% by volume. These adhesives are placed in the bondline, and, upon application of a suitable field, the particles cause the adhesive to cure and create a weld. Higher frequencies (> 100 kHz) are required to heat the small magnetic particles that are mixed into our induction welding implants.

2.3 Carbon-Fiber Composites. Due to the electrically conductive nature of carbon fibers, carbon-fiber composites can be heated by induction without the use of susceptors to translate the electromagnetic energy into thermal energy. Our previous research has shown that the primary heating mechanism is the dielectric loss at junctions of fiber overlap between layers of the composite [7-9]. This also implies that unidirectional carbon-fiber composites will show minimal heating. A schematic of the heating mechanism is shown in Figure 5.

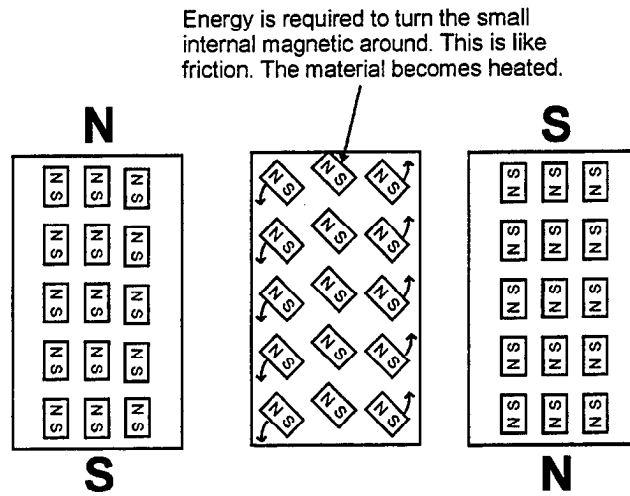


Figure 3. Model of Magnetic Domains During Hysteresis Loss.

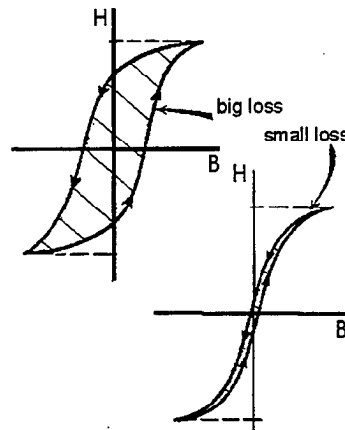


Figure 4. Hysteresis Loops in Ferromagnetic Materials.

The carbon-fiber heating phenomenon can be used for a variety of applications, such as nonautoclave cure of carbon-fiber thermosets, rapid processing of carbon-fiber thermoplastics, repair using carbon-fiber prepreg systems, etc. As described in our earlier report [10], the SERDP-funded program will take advantage of our unique knowledge of these mechanisms to demonstrate the applicability of induction heating to near elimination of hazardous waste in the production of the Army's M829E3 composite sabot.

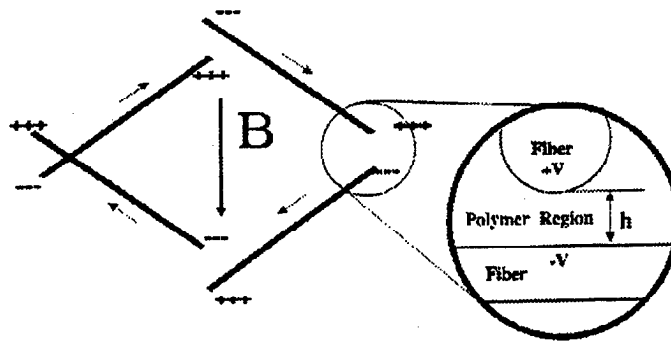


Figure 5. Schematic of Heating Mechanism in Carbon-Fiber-Based Composites [7].

2.4 Induction Heating System. The induction heating system used in these studies is composed of the induction heater unit, an infrared (IR) camera, several National Instruments SCXI components, a digital data acquisition board, and a control computer. A National Instruments LabVIEW software interface has been developed for data acquisition and control of the induction heating system. IR images are acquired and processed in real time to determine the thermal history of the composite part. Control of the induction heater is achieved through a proportional integral differential (PID) controller, where the user provides the desired part temperature and heating rate.

Figures 6 to 8 show a comparison of open-loop response (known constant power setting to achieve the setpoint), manual control (two different trials to reach the setpoint temperature as rapidly as possible with small overshoot), and the response from PID control of the system. Manual control allows for a reduced time to dwell temperature than open-loop fixed-power heating. However, manual control procedures generally exhibit undesirable overshoot and variability in the process. When Figure 8 is compared with Figures 6 and 7, it is apparent that our PID-based control provides sufficient time-to-dwell and low-variability features.

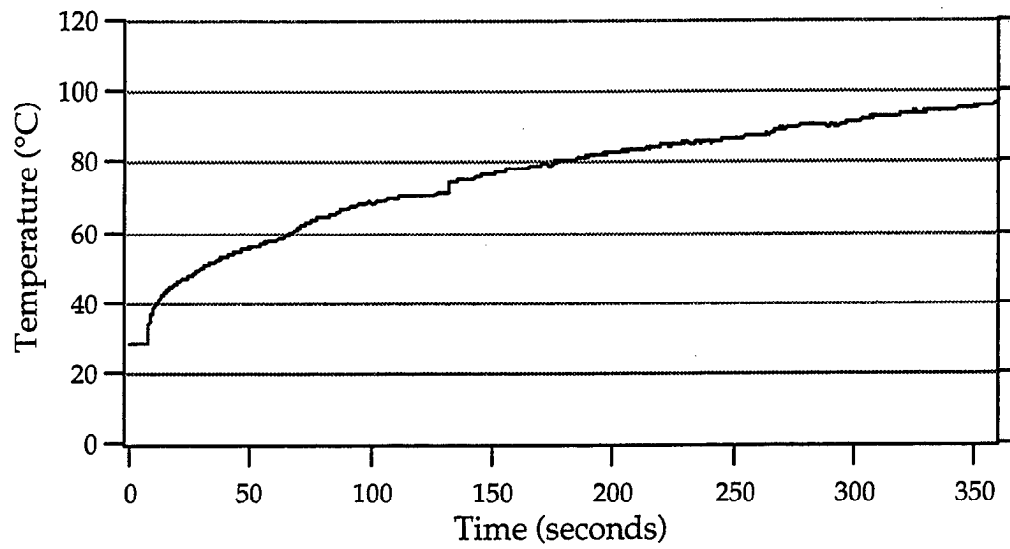


Figure 6. Open-Loop Response of Induction Heating System.

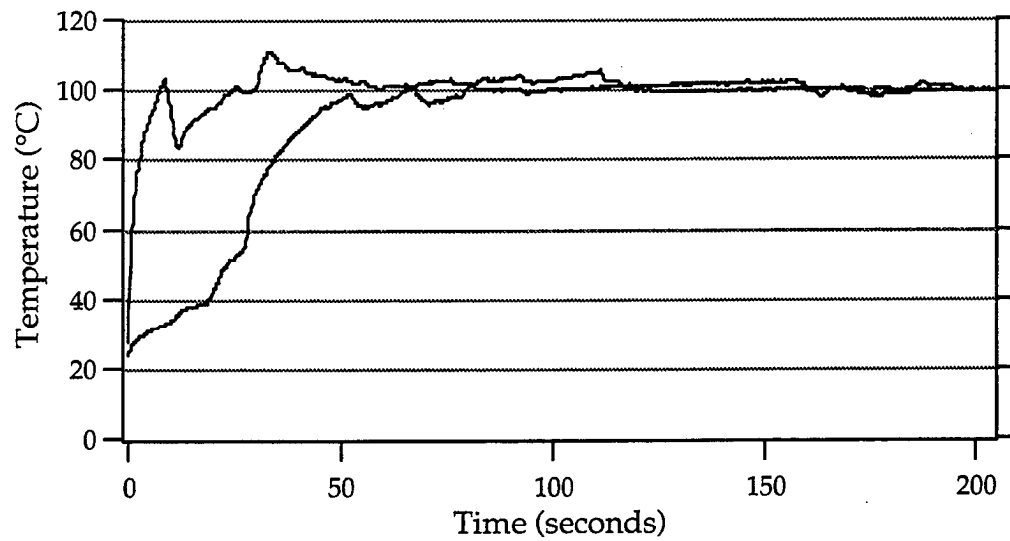


Figure 7. Induction Heater Response With Manual Control.

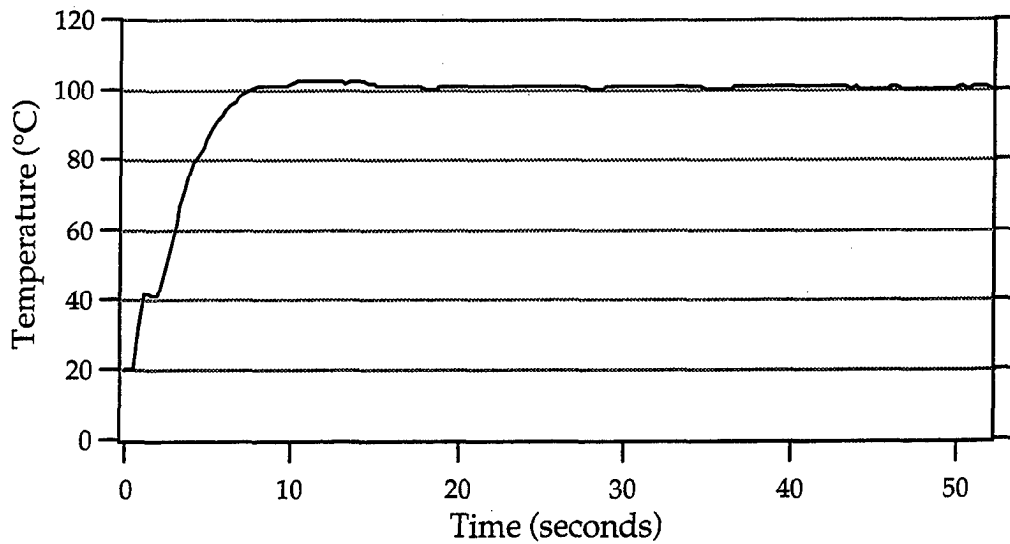


Figure 8. Induction System Response With PID Feedback Control.

3. Induction-Based Accelerated Cure of Adhesives

The increasingly widespread use of composite materials in defense and aerospace applications has resulted in an urgent need for fast and efficient field and depot-level repair techniques for these components. Usually, repairs use an adhesively bonded patch over the damaged area. Proper curing of the adhesive used in the repair is crucial to the integrity and strength of the repaired component. Although room-temperature-curing adhesives have been extensively used in many repair applications, they have the disadvantage that complete curing often requires many hours or days. The time to complete cure can be reduced by application of heat to the patch, usually by the use of heat blankets or heat lamps. However, these methods are inefficient and, in some cases, insufficient, since substantial heat is inevitably lost to the surrounding material and environment. Induction heating, on the other hand, enables local and rapid heating of the area close to the adhesive bondline.

As described in Fink et al. [10], not only are there significant environmental advantages related to the development of infinite-storage induction-curable repair adhesives, but another

significant advantage is the ability of induction-based curing to rapidly heat and cure the adhesive under vacuum conditions, significantly reducing VOC emissions. Additionally, induction-based heating eliminates the need for NO_x-generating autoclaves for thermally cured repairs.

3.1 Characterization of Cure Kinetics. To ensure proper curing of adhesives using induction heating, it is necessary to establish appropriate process windows. The process window is then used to optimize the bonding process with respect to temperature and time. Factors that dictate the process window include cure kinetics, evolution of exotherms, flow and wetting, and thermally induced residual stresses. Adhesive cure kinetics is the most dominant factor and must be addressed to determine cure time as a function of temperature, as well as ultimate degree of cure. A typical room-temperature-curing epoxy system (Hysol EA9394) was chosen for evaluation of accelerated-cure properties. It is a two-part epoxy room-temperature-curing paste adhesive with a suggested cure time of 3 to 5 days at room temperature, making it an ideal candidate for accelerated cure studies.

Differential scanning calorimetry (DSC) was used to characterize the cure kinetics of the thermosetting polymer [6, 11]. Since the heat evolution dQ/dt measured by the DSC results from the chemical cross-linking reaction, it is possible to relate the heat evolution dQ/dt to the rate of reaction $d\alpha/dt$ and the conversion α . This can be accomplished by using the following relationships:

$$\frac{d\alpha}{dt} = \frac{1}{\Delta H_{tot}} \left(\frac{dQ}{dt} \right)_t \quad (1)$$

and

$$\alpha = \frac{1}{\Delta H_{tot}} \int_{t_0}^t \left(\frac{dQ}{dt} \right)_t dt, \quad (2)$$

where ΔH_{tot} is the total heat of reaction, generally determined by averaging the reaction exotherms measured from several dynamic temperature DSC runs. Various chemical kinetic models can then be fit using data obtained from isothermal DSC experiments.

The mechanistic models of thermoset cure that usually provide a more accurate representation of cross-linking reactions are not generally applicable to complex systems such as formulated adhesives. Since the goal is to provide a process window for accelerated cure, the specific cure mechanisms need not be critically assessed. Alternatively, several empirical models have been successfully used to predict curing of thermosetting polymers. One popular model proposed by Kamal and Sourer [12] that has found widespread acceptance for a number of cross-linking reactions (including epoxies) is shown as equation (3) and will be used to fit the adhesive studied here.

$$\frac{d\alpha}{dt} = (k_1 + k_2\alpha^m)(\alpha_u - \alpha)^n \quad (3)$$

In equation (3), α is the degree of conversion, α_u is the temperature-dependent maximum conversion, k_1 and k_2 are Arrhenius-type rate constants, and m and n are constants usually assumed to sum to 2 but are often allowed to vary freely. The α_u term arises from the fact that the entire heat of reaction is not released during isothermal cure due to the decreased mobility of the polymer chains as cross-linking occurs. Performing a series of isothermal cures enables values for the model parameters to be determined and used to predict the cure kinetics of the adhesive.

Fifteen dynamic DSC runs were performed to evaluate ΔH_{tot} of the adhesive. The epoxy (part A) and hardener (part B) were mixed in the recommended ratios by weight before being immediately inserted into the DSC (TA Instruments 2908), where they were heated at 10°C/min from 0°C to 200°C. The resulting cure exotherm was integrated to evaluate the heat of reaction. The average and standard deviation of ΔH_{tot} was 354.8 ± 14.7 J/g. This average value is used in equations (1) and (2) to relate the isothermal heat data to α and $d\alpha/dt$.

Isothermal DSC runs were also performed at temperatures ranging from 80°C to 160°C. Samples of adhesive and hardener were mixed and placed in the preheated DSC cell. Data were collected until the heat flow returned to the baseline value. The isothermal heat flow was related to α and $d\alpha/dt$ using equations (1) and (2). Equation (3) was then used to fit the $d\alpha/dt$ vs. α curves for each isotherm. A residual DSC run at 10°C/min from 0°C to 200°C followed each isothermal DSC run. A value of α_u was determined from

$$\alpha_u = 1 - \frac{\Delta H_{res}}{\Delta H_{tot}}, \quad (4)$$

where ΔH_{res} is the residual heat of reaction. The parameters m and n were permitted to vary freely. Analysis of each experiment produces values for all of the kinetic parameters at that specific temperature. In general, it was found that equation (3) enabled reasonably good fit of the data, the fit being better at higher temperatures. Analysis of the data indicated that k_1 is nearly constant, regardless of temperature. The parameters are summarized in Table 1.

Table 1. Cure Kinetics Model Parameters for Hysol EA9394

| Parameter | Value |
|------------|--|
| k_1 | 0.120 ± 0.107 |
| k_2 | $4.098 \times 10^6 \exp(-5533.9/T(K))$ (1/min) |
| M | 0.593 ± 0.070 |
| N | 1.407 ± 0.073 |
| α_u | $0.712 + 1.8 \times 10^{-3} T$ (°C) |

The model enables prediction of the entire curing process over a wide range of processing temperatures. The prediction of cure time at a specific temperature is of greatest interest to the application of induction techniques to accelerate adhesive cure. Figure 9 shows model predictions for cure time compared to the experimentally observed cure times. A family of curves is generated for the range of values of α from 0.7 to 0.99. Here, cure time is defined as the amount of time necessary to reach the specified value of α for each temperature. It is seen that, at the lower temperatures, it is not possible to attain high values of α . For example, at

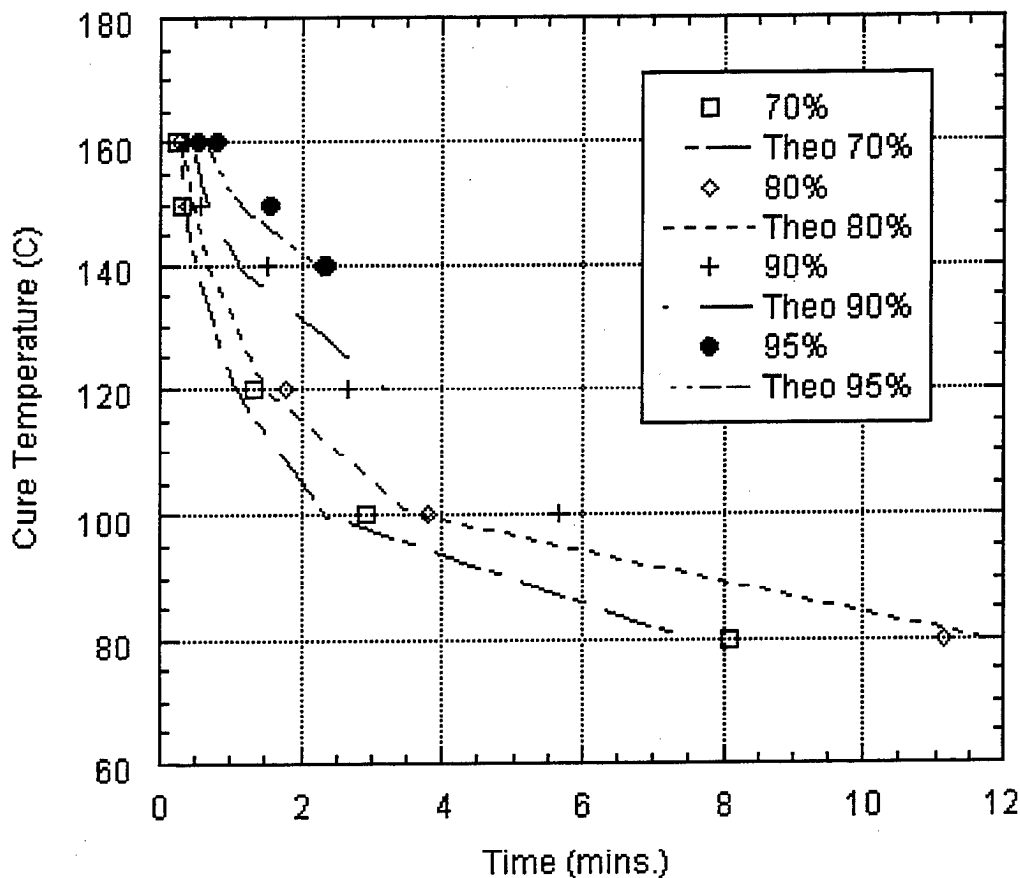


Figure 9. Comparison of Kinetics Model Cure Times to Experimental Cure Times for Varying Degrees of Cure.

100°C it is not possible to obtain a value of α greater than 0.9. If a greater degree of cure is desired, it is necessary to increase the cure temperature to about 140°C. The curves also show that the times to cure are generally very short, particularly at the higher temperatures. Above 140°C, a value of α of 0.95 could be achieved within 2 min. At the relatively low temperature of 80°C, it took less than 12 min to achieve a value of α of 0.8. This is comparable to the value of α_u of 0.79 for the adhesive when cured at room temperature for 120 hr. The results were used to determine process windows for the induction-assisted accelerated cure of this adhesive.

To compare nominal strengths and study the effect of a susceptor material in the bondline, several types of single-lap shear (SLS) specimens were fabricated according to the American Society for Testing and Materials (ASTM) standard D1002. The adherends were satin-weave glass/epoxy. A panel consisting of 34 plies of prepreg was prepared in an autoclave and cured according to the manufacturer's recommendations. The 3.0-mm-thick cured panel was cut into pieces of adherends, each measuring 102 mm × 25 mm (4 in × 1 in). Eight cases of SLS specimens under various curing conditions were fabricated (Table 2). Case A represents the condition for use of the adhesive as recommended by the manufacturer. In each of cases C to H, the susceptor embedded in the adhesive layer was a copper mesh with a wire density of 30 × 30 per in² and wire diameter of 0.15 mm (0.006 in). This mesh was chosen from preliminary tests of SLS specimens using this mesh, which showed reasonable shear strengths compared to similar tests using various other mesh densities and metal types.

Table 2. Lap Shear Data for Hysol EA9394

| Case | Adhesive Curing Process | Number of Specimens Tested | Mean Nominal Shear Strength and Standard Deviation (MPa) | Coefficient of Variation (%) |
|------|---|----------------------------|--|------------------------------|
| A | Room-Temperature-Cured for 120 hr Without Susceptor | 7 | 14.8 ± 1.0 | 6.76 |
| B | Oven-Cured at 160°C for 1 hr Without Susceptor | 4 | 18.1 ± 2.1 | 11.60 |
| C | Room-Temperature-Cured for 120 hr With Copper Susceptor | 5 | 12.3 ± 0.9 | 7.32 |
| D | Oven-Cured at 100°C for 1hr With Copper Susceptor | 4 | 14.7 ± 0.6 | 4.08 |
| E | Oven-Cured at 160°C for 1 hr With Copper Susceptor | 4 | 13.2 ± 0.6 | 4.54 |
| F | Induction-Cured at 100°C for 15 min With Copper Susceptor | 6 | 15.2 ± 0.7 | 4.60 |
| G | Induction-Cured at 160°C for 10 min With Copper Susceptor | 6 | 14.3 ± 0.8 | 5.59 |
| H | Induction-Cured at 100°C for 15 min With Copper Susceptors (Double Notch Shear Specimens) | 6 | 16.9 ± 0.7 | 4.14 |

The copper mesh was cut into rectangular strips of 25.4 mm × 12.7 mm (1 in × 0.5 in) and wetted with the mixed adhesive on both sides before being placed in the bond area. The corresponding mating surfaces of the adherends were also applied with the adhesive by means of a wooden applicator. In each case, vacuum consolidation was used to ensure uniformity of applied pressure and adhesive bondline thickness between specimens. The SLS specimen was secured onto a base plate with Kapton tape. A support plate of thickness equal to that of the adherend was used to support the top adherend as it was bonded to the bottom adherend. A piece of bagging film was placed onto the arrangement and sealed on all four edges of the base plate with tacky sealing tape. Vacuum was drawn from the interior via a plastic hose. When the vacuum pressure was applied, excess adhesive was immediately squeezed out from the sides of the SLS specimen. After the adhesive had cured or hardened, the excess adhesive was removed by filing off the edges of the SLS specimen.

Cases A–E are baseline cases. In cases B, D, and E, where the adhesive in the specimens was cured at elevated temperatures while still under vacuum consolidation, the entire setup was placed in a conventional oven, which was preheated to the desired temperature (either 100°C or 160°C), for at least 1 hr. The oven has an outlet that enables the plastic hose to be drawn out of the chamber and connected to the vacuum pump.

In cases F, G, and H, where the adhesive was cured by induction heating, the entire setup was held vertical by a vice grip attached to one end of the base plate and placed in between an induction coil shaped like an earmuff, as shown in Figure 10. The induction unit was capable of generating a peak-to-peak current of between 0 and 55 amp at a frequency of 284 kHz. A thermal camera was positioned in front of the setup to capture the full-field surface temperature of the bonded area as the induction heating proceeded. The data were fed to a computer and displayed in real time on a color monitor. The temperature tended to be a little higher at the edges and corners of the bond area initially, but after about 20 s, the temperature distribution became very uniform throughout the bond area. A typical temperature profile with time at the center of the bond area is shown in Figure 11. In Table 2, the selected process windows of 10

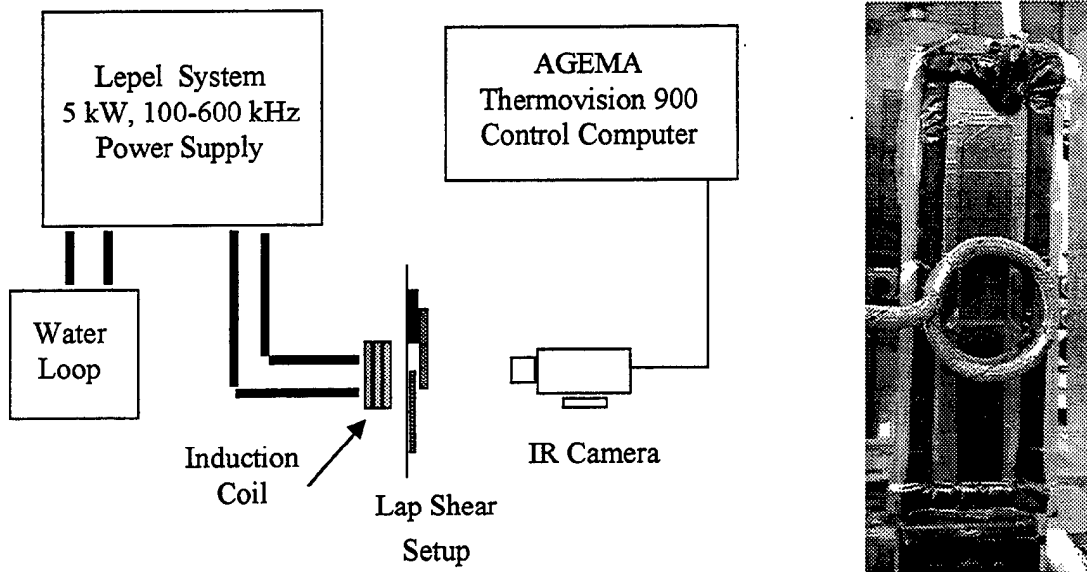


Figure 10. SLS Specimen Fabricated Setup With Copper Wire Mesh Susceptors and Hysol EA9394 Adhesive.

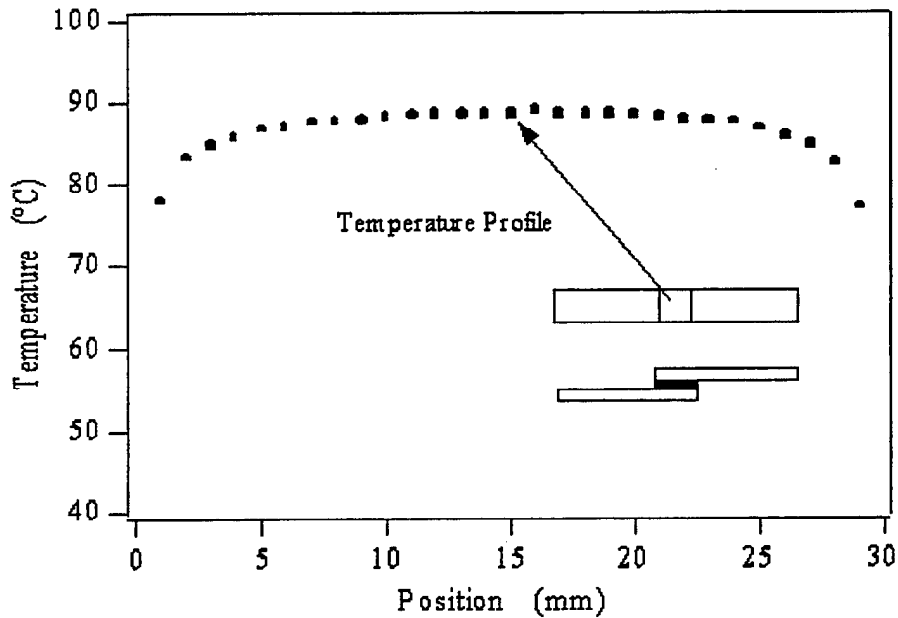


Figure 11. Temperature Profile of SLS Specimens Demonstrating Uniformity of Heating in Process Window Enabled by Induction Heating for Repair.

and 15 min for cases F and G, respectively, were guided by the cure kinetics study described earlier.

3.2 Performance Comparison of Adhesive Systems. All SLS and DNS specimens were tested to failure in an Instron universal testing machine. The mean nominal shear strengths and associated standard deviations are given in Table 2. The results are plotted in Figure 12, where values of the mean ± 3 standard deviations are used. Interestingly, the presence of the copper susceptor seems to reduce the scatter of the data, as shown by comparing the standard deviation values of cases A and B with those of cases C and E. Indeed, all the cases of SLS specimens with susceptors (C, D, E, F, G, and H) have lower coefficients of variation. In a typical failed SLS specimen that has been cured by induction, although the adhesive layer had failed, the mesh susceptor was still partially attached to both adherends. The maximum load was reached just prior to sudden cohesive failure of the adhesive layer. This value of load is used to compute the nominal shear strength of the specimen in Table 2. After fracture of the adhesive layer, the specimen was still able to support a small load due to the copper susceptor. On subsequent application of load, the copper wires eventually fractured, but approximately half of the mesh remained attached on each adherend. The presence of the susceptor provided alternative crack paths through the adhesive layer and in between the spaces within the mesh. The overall effect may be a decrease in sensitivity to microvoids or defects in the adhesive layer, leading to less scatter in the strength data.

Elevated-temperature cure at 160°C for specimens without susceptors (compare cases A and B) increases the shear strength but also significantly increases the amount of scatter in the data. For room-temperature-cured adhesives, inclusion of a susceptor decreases the average nominal shear strength (cases A and C). This probably due to the increase in bondline thickness, although a stress analysis of an SLS joint containing a susceptor layer has not yet been carried out. Elevated-temperature-cures at 100°C and 160°C for specimens with susceptors show improvement in nominal shear strengths, regardless of whether the heat was supplied in a conventional oven (cases D and E) or through induction heating (cases F and G). Significantly, in both methods of heating, the average strength of specimens cured at 100°C is higher than that

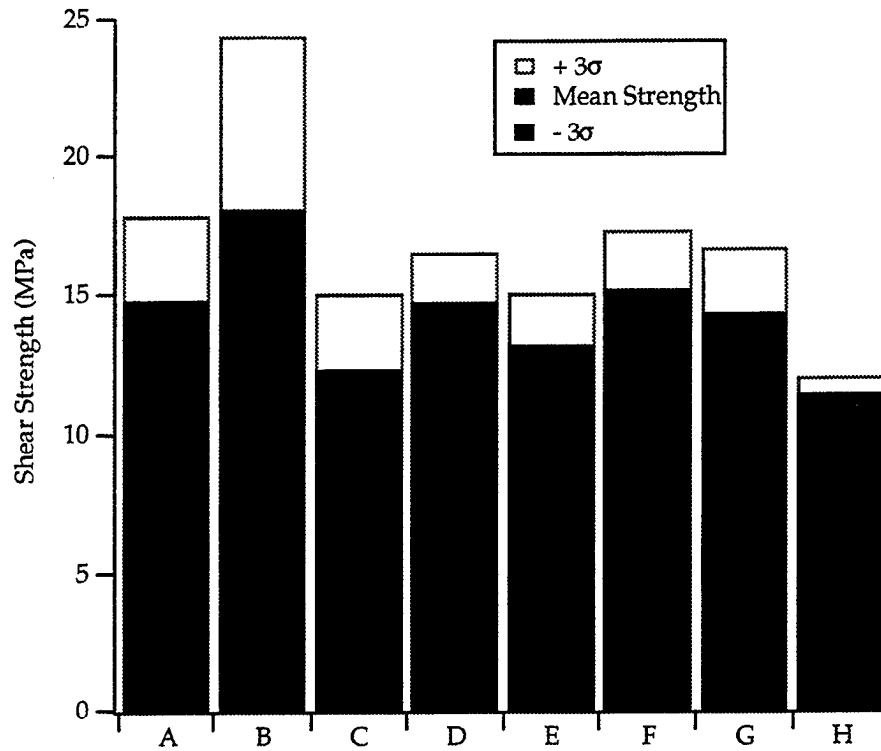


Figure 12. Plot Showing $\pm 3\sigma$ Performance of SLS Specimens.

of specimens cured at 160°C. It appears that there is an optimal elevated curing temperature above which the strength will begin to decrease. An increase in α_u with temperature would result in an increase in resin strength but also a reduction in fracture toughness. Consequently, the stress-state in the specimen due to the mechanical loads is unchanged. Specimens cured at 100°C may be less notch-sensitive due to the higher toughness than specimens cured at 160°C.

It is concluded that induction heating can be successfully used to accelerate the curing of room-temperature-cure adhesives at elevated temperatures, since the results did not show substantial reduction in the joint strength of induction-cured specimens. For the adhesive used in this study, curing time was reduced from 120 hr to 15 min.

4. Induction-Based Repair of Integral Armor

Initial studies were performed to assess the applicability of induction-based repair of the Army's composite integral armor using metal mesh susceptors. Desirable repair features for composite armor can be summarized as follows:

- one-step process for multilayer repair,
- one-sided access,
- vacuum consolidation,
- gap-filling process,
- variable damage area capability,
- rapid portable process, and
- able to renew structural, ballistic, and signature performance.

The induction-based repair system can address all of these requirements, in addition to using adhesive systems that have no shelf-life requirements. Figure 13 shows a section of a typical composite armor panel for land vehicles.

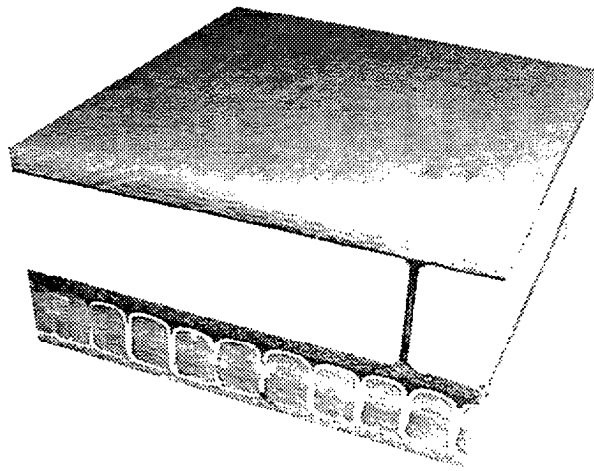


Figure 13. Section of Typical Multilayered Multifunctional Composite Armor Panel.

4.1 Susceptor and Coil Design. For bonding integral armor components, two mesh types were used.

(1) Copper Mesh: 30 × 30 mesh
0.006-in diameter
crosswire cloth

(2) Steel Mesh: 30 × 30 mesh
0.0065-in diameter
crosswire cloth

Initial experiments focused on heating a ceramic tile, with different coils positioned on one side and the mesh fixed on the other side with Kapton tape, under vacuum pressure. These experiments showed that the steel mesh was heating up faster than the copper mesh and required a lower power setting to reach adequate temperatures for adhesive cure. Greater heating for the same power translates to higher depth of penetration, which means that thick composite parts can be heated through as required for armor repair, where the adhesive to be heated is displaced from the outer surface. Figure 14 shows the temperature profile of a ceramic tile/mesh under vacuum with a conical coil. The temperature differential between the center and the outside of the tile (~ 35°C) is greater than allowable for adhesive repair.

4.2 Coil Motion Studies. Temperature differentials can be reduced by coil design, coil motion, or mesh susceptor design. Coil and mesh designs are in progress to reduce this differential as much as possible. One technique to achieve more uniform temperatures is to use a moving coil. An ABB robot system with 6 degrees of freedom was used for this purpose. The coil was mounted on the robot head using a plexiglass attachment. Several different motion patterns were examined to determine the optimal coil motion for uniform temperatures in the ceramic tile system. Figure 15 shows comparisons of heating profiles without and with motion, respectively, and demonstrate the ability of coil motion in improving the uniformity of temperatures in the mesh. Figure 16 shows the actual temperature along the lines marked in Figure 15. The temperature differential is reduced from 40°C to 10°C in the plane of the mesh susceptor.

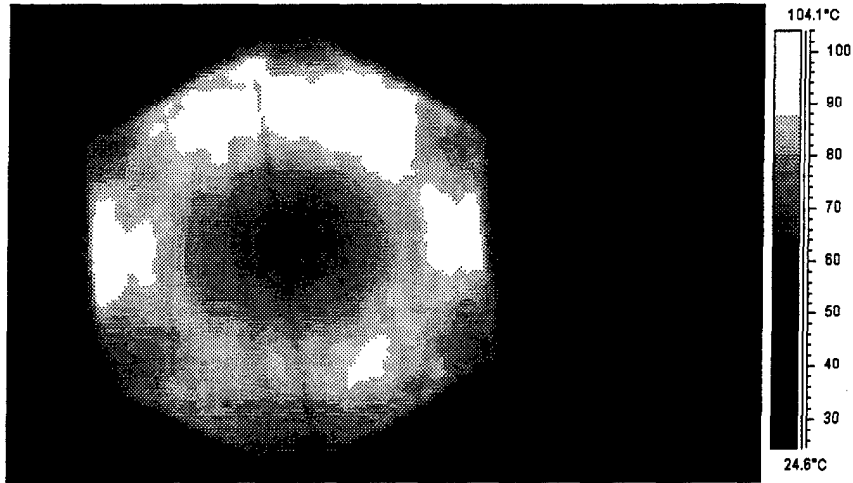


Figure 14. Temperature Profile of Ceramic Tile/Steel Mesh.

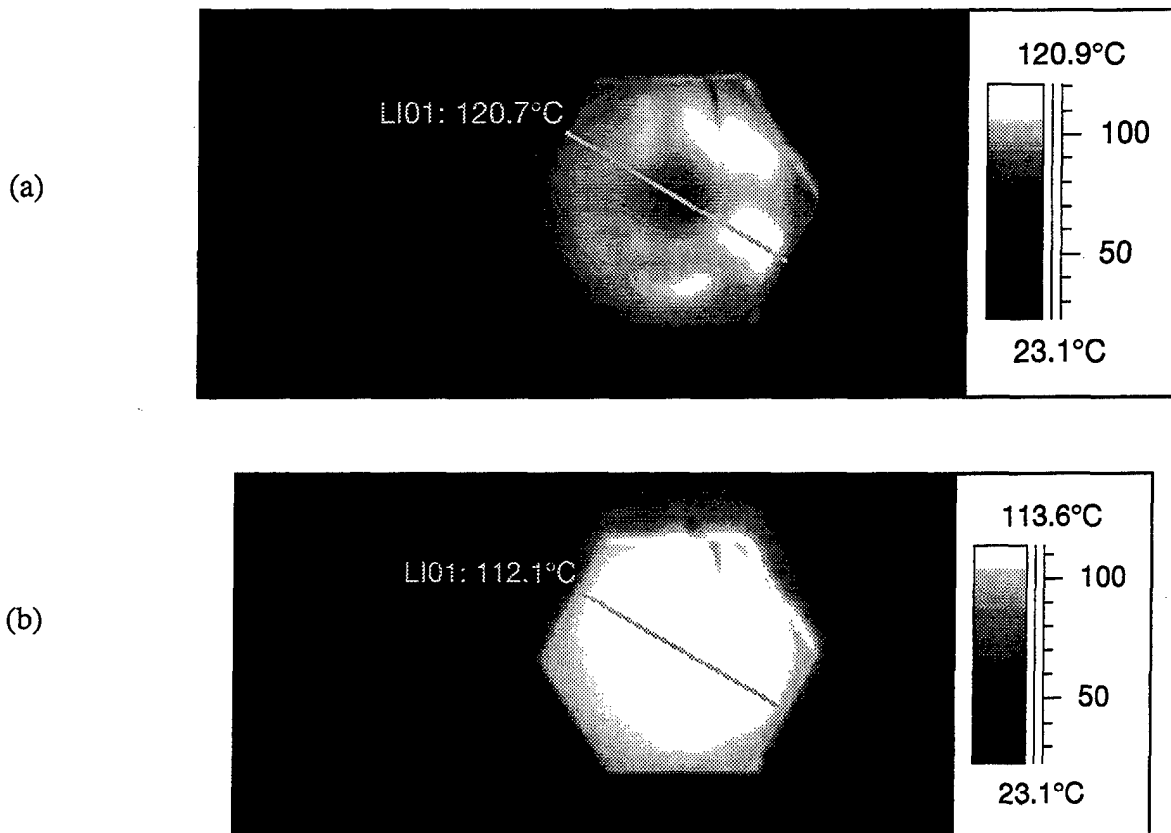


Figure 15. Comparison of Temperature Profiles After 20 min of Heating (a) Without Coil Motion and (b) With Coil Motion.

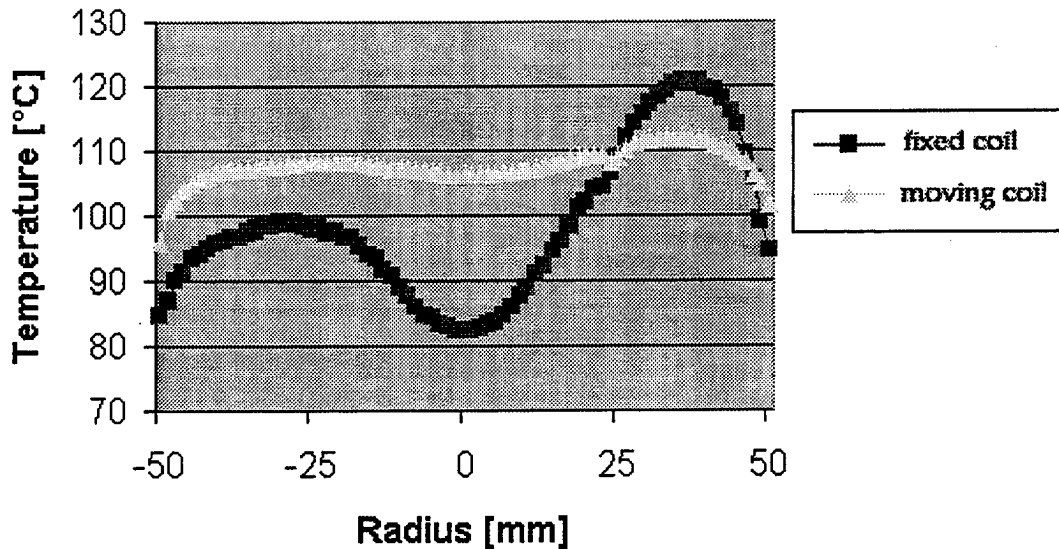


Figure 16. Temperatures of Lines LI01 in Figure 15.

4.3 Composite Armor Subsystem Bonding. Viewed simplistically, composite armor consists of four basic subsystems:

- (1) thin facesheet (graphite/epoxy or glass/epoxy),
- (2) ceramic tile for ballistics,
- (3) rubber layer to absorb tile fragments, and
- (4) thick composite layer for structure and ballistics.

Repair of armor after ballistic impact typically involves replacing the first three layers or subsystems. For demonstration purposes, the current effort focused on single-step and multi-step bonding of all subsystems using steel mesh susceptors with the Hysol EA9394 adhesive system and the coil configuration described in the previous sections. The following materials were chosen as representative of the four subsystems:

- (1) thin facesheet—1/8-in fiberglass/epoxy,
- (2) ceramic tile—11/16-in ceramic,

- (3) rubber layer—1/16-in rubber, and
- (4) thick composite layer—7/16-in fiberglass/epoxy.

Initially, the influence and behavior of each subsystem or each part to its neighboring part during induction heating was examined. The bonding test sequence was as follows:

- (1) bonding a 1/8-in fiberglass and a 1/16-in rubber sample,
- (2) bonding a 1/16-in rubber layer and 11/16-in ceramic tile,
- (3) bonding a 11/16-in ceramic tile and 7/16-in fiberglass, and
- (4) bonding thin fiberglass/rubber/ceramic/thick fiberglass in one step.

The first three experiments produced the necessary data about power requirements for heating each subsystem/neighbor up to the curing temperature of the adhesive. In addition, the temperature difference between the adhesive layer and the top surface (IR camera) was determined by placing thermocouples at the adhesive layer. When composite subsystems are bonded, the IR camera measures surface temperatures and not the bondline temperatures. Therefore, it is necessary to establish temperature differentials between the surface and the bondline when two or more subsystems are bonded, so that the adhesive at the bondline does not overheat and degrade.

In all the bonding tests, the coil was moved along the pattern developed during coil motion studies, and the adhesive was heated to a temperature of $100 \pm 10^\circ\text{C}$ at the bondline. Table 3 and Figure 17 show the results of bonding an 11/16-in-thick ceramic tile to a 7/16-in composite panel. A frequency of 351 kHz was applied for 20 min. The coil was moved about the test specimen in a circular motion around the center of the tile.

4.4 One-Step Multilayer Composite Bonding. The final experiment was to bond all four subsystems together in a single step. This would simulate an actual repair procedure of a multilayered multifunctional composite armor panel. The four subsystems bonded were

| Temperature Reading of IR Camera | | | | |
|----------------------------------|--------|--------|---------|--------------|
| Thermocouple position | Spot 1 | Spot 2 | Hotspot | Thermocouple |
| Backside of fiberglass | — | — | 143 | — |
| Mesh | 77.8 | 84 | 117.2 | 117.1 |

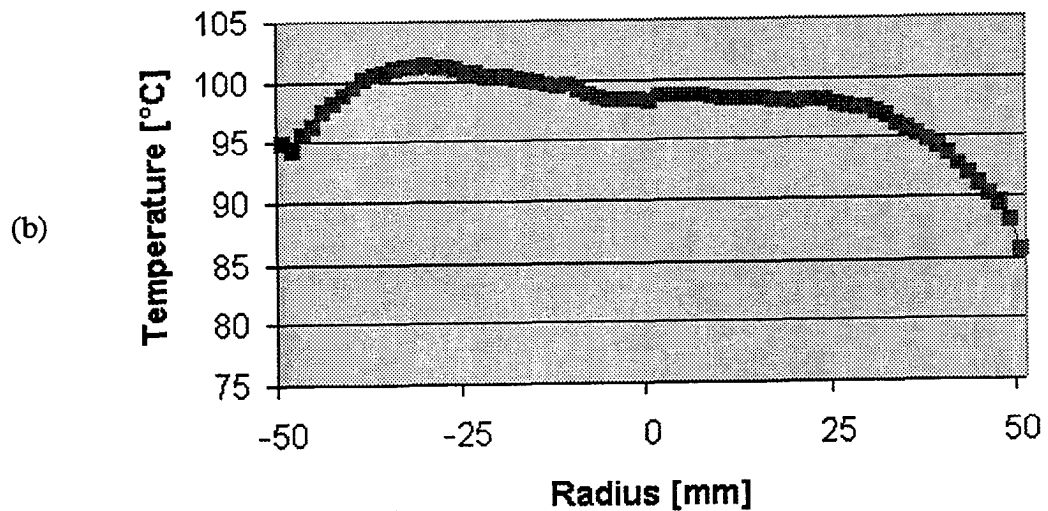
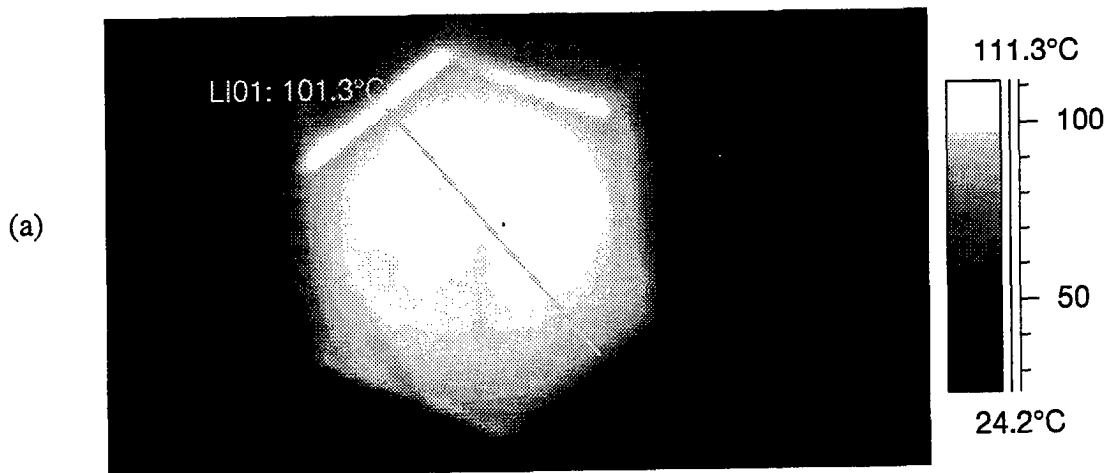


Figure 17. Surface Temperature Variation During Bonding of Ceramic Tile to 7/16-in-Thick Glass/Epoxy Composite With Coil Motion.

- (1) thin facesheet—1/8-in fiberglass/epoxy,
- (2) ceramic tile—11/16-in ceramic,
- (3) rubber layer—1/16-in rubber, and
- (4) thick composite layer—7/16-in-thick fiberglass/epoxy.

Figure 18 shows a schematic of the lay-up for this process. A layer of mesh/adhesive was placed between each subsystem, resulting in three adhesive layers or bondlines, as shown in Figure 18. The layers were placed on a backing sheet and vacuum-bagged for consolidation pressure. The same coil and motion pattern was used as before. The coil is a one-sided conical coil, which is necessary for field repair applications because it is not always possible to access both sides of the part to be repaired. A coil frequency of 351 kHz was applied for 20 min.

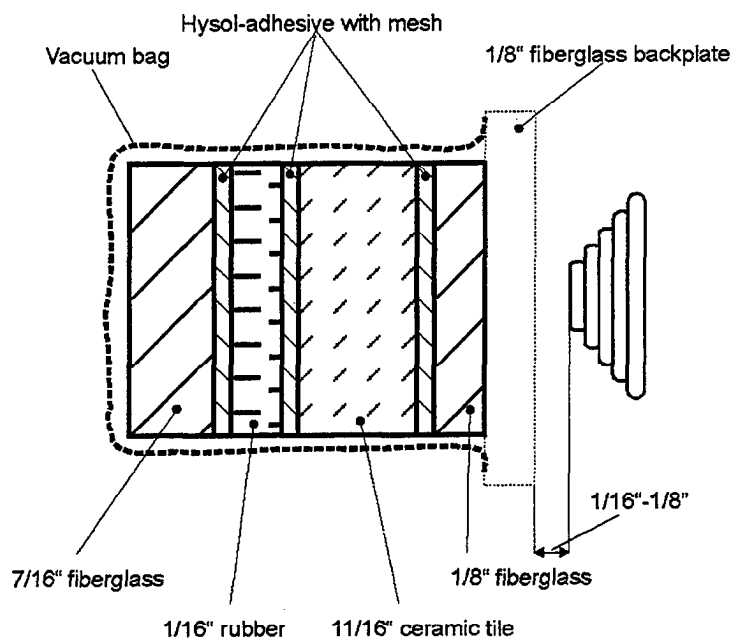


Figure 18. Schematic of Lay-Up Sequence for One-Step Induction Repair of Composite Armor Panel.

Temperature profiles of the surface during the heating process are shown in Figures 19 and 20. Surface temperatures are fairly uniform, except at the edges of the part. However, in a realistic repair scenario, there will be no edges as seen in this case, since the repair fills in a

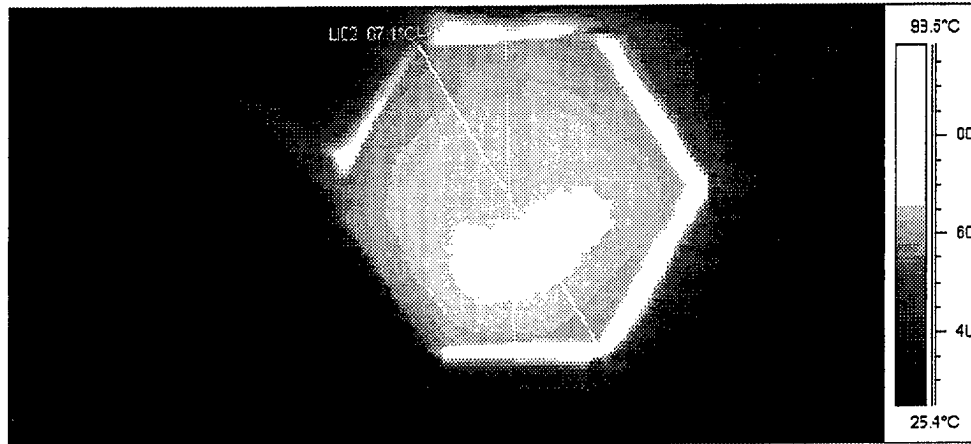


Figure 19. Surface Temperature Profile for Single-Step Bonding With Coil Motion.

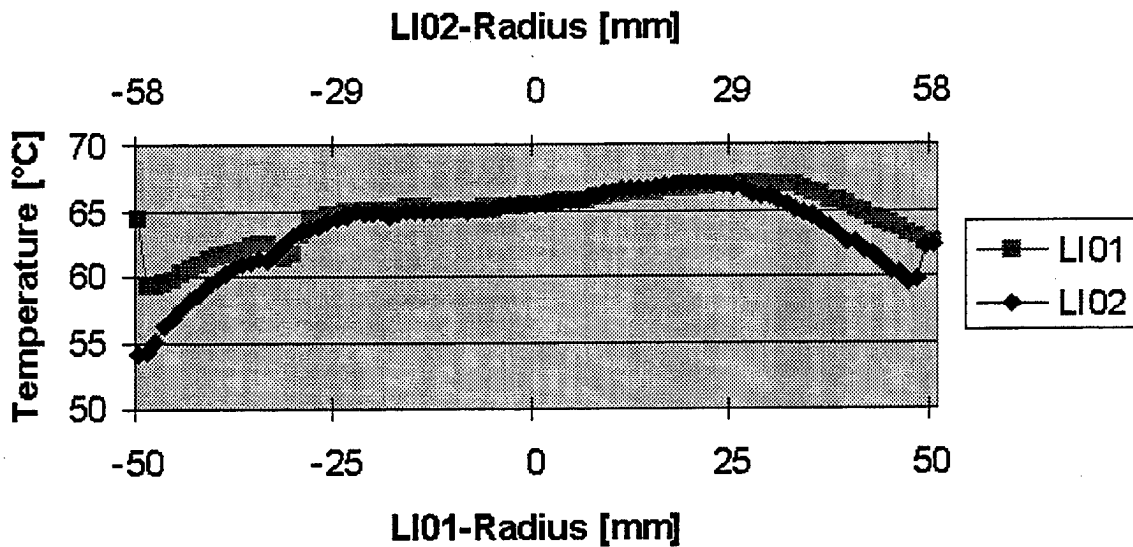


Figure 20. Surface Temperature Variation at Two Different Locations.

damaged area. One of the primary challenges was to ensure similar temperatures in all three bondlines, despite the different distances from the coil. The thermal properties of each subsystem were important for this, and the high thermal conductivity of the ceramic tile played a significant role in maintaining similar temperatures across the bondlines.

With IR spot locations provided in Figure 21, the time-temperature response during the heating process is shown in Figure 22. The entire process took approximately 30 min, which demonstrates the rapidity of the process. During this process, a heating depth of up to 1.25 in was demonstrated. Greater depths are possible and are the subject of future investigations. Figure 23 shows a photograph of the final bonded sample with the multiple layers. Good-quality bondlines were obtained at all three interfaces.

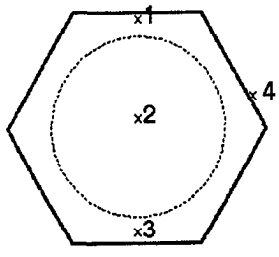


Figure 21. Spot Locations for IR Camera Temperature Measurement.

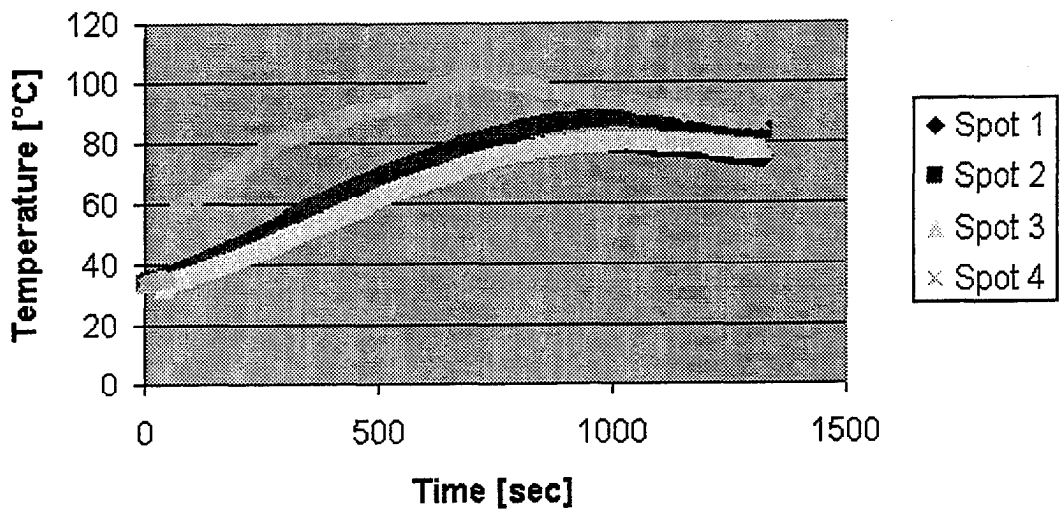


Figure 22. Time/Temperature Response During One-Step Induction Bonding as Measured by IR Camera.

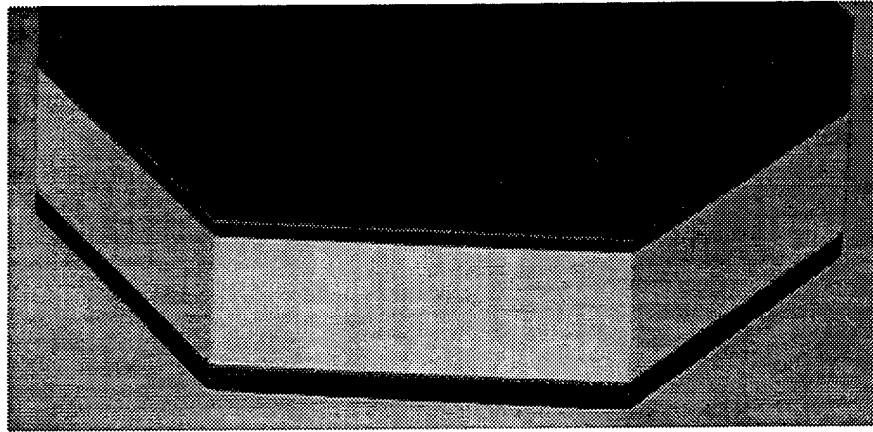


Figure 23. Single-Step Bonded Multilayer Composite Specimen.

5. Conclusions

The current work has established that induction heating using conductive mesh susceptors can be used to rapidly cure thermosetting adhesives under a VOC-reducing vacuum condition. It has also been established that the presence of these susceptor materials, although not optimized, does not adversely affect the mechanical performance of the bondline when considering the low scatter in lap shear strength. The feasibility of induction-based repair using metallic screen susceptors has been demonstrated. The applicability of induction heating to multilayer single-step bonding has further been demonstrated, wherein heat generation is limited to localized bondline regions, allowing optimization of repair processes. Much work is needed to optimize both the susceptors and the resin systems. Optimization of the process should be paralleled with more aggressive strength and durability testing.

INTENTIONALLY LEFT BLANK.

6. References

1. Fink, B. K., S. H. McKnight, J. W. Gillespie, Jr., and S. Yarlagadda. "Nano-Particulate and Conductive Mesh Susceptors for Induction-Based Repair of Composites." *Proceedings of the 21st Army Science Conference: Science and Technology for Army After Next*, Norfolk, VA, 15–17 June 1998.
2. Tay, T. E., S. Yarlagadda, B. K. Fink, and S. H. McKnight. "Application of Induction Heating to Accelerate Curing of Adhesives in Bonded Joints." *Proceedings of American Society for Composites Thirteenth Technical Conference*, Baltimore, MD, 21–23 September 1998.
3. Firko, J., S. Yarlagadda, J. W. Gillespie, Jr., and B. K. Fink. "Optimization of Heat Generation in Induction Bonding Using Metal Mesh Susceptors." *Proceedings of American Society for Composites Thirteenth Technical Conference*, Baltimore, MD, 21–23 September 1998.
4. McKnight, S. H., B. K. Fink, S. Wells, S. Yarlagadda, and J. W. Gillespie, Jr. "Accelerated Curing of Epoxy Paste Adhesives for Repair of Composites Using Induction Heating." *Proceedings of ANTEC 98*, Society of Plastics Engineers, Brookfield, CT, 1998.
5. Tay, T. E., S. Yarlagadda, J. W. Gillespie, Jr., B. K. Fink, and S. H. McKnight. "Accelerated Curing of Adhesives in Bonded Joints by Induction Heating." *Journal of Composite Materials*, in press.
6. Yarlagadda, S., J. W. Gillespie, Jr., and B. K. Fink. "Resistive Susceptor Design for Uniform Heating during Induction Bonding of Composites." *Journal of Thermoplastic Composite Materials*, vol. 11, no. 4, pp. 321–337, July 1998.
7. Fink, B. K., R. L. McCullough, and J. W. Gillespie, Jr. "A Local Theory of Heating in Cross-ply Carbon Fiber Thermoplastic Composites by Magnetic Induction." *Polymer Engineering and Science*, vol. 32, no. 5, pp. 357–369, March 1992.
8. Fink, B. K., J. W. Gillespie, Jr., and R. L. McCullough. "Induction Heating of Cross-Ply Carbon Fiber Thermoplastic Composites." *Proceedings of ANTEC 92*, Society of Plastics Engineers, Brookfield, CT, 1992.
9. Fink, B. K., J. W. Gillespie, Jr., and R. L. McCullough. "Heating of Continuous Carbon Fiber Thermoplastic Composites by Magnetic Induction." *Proceedings of the Third DOD/NASA Repair Technology Workshop*, 1991.

10. Fink, B. K., S. H. McKnight, C. H. Newton, J. W. Gillespie, Jr. and G. R. Palmese. "Non-Polluting Composites Repair and Remanufacturing for Military Applications: An Environmental and Cost Savings Analysis." Technical Report, Strategic Environmental Research and Development Program Office, Alexandria, VA, September 1998.
11. McKnight, S. H., B. K. Fink, S. Wells, S. Yarlagadda, and J. W. Gillespie, Jr. "Accelerated Curing of Epoxy Adhesives for Repair of Composites Using Induction Heating." *Proceedings of ANTEC 98*, Society of Plastics Engineers, Brookfield, CT, 1998.
12. Kamal, M. R. and S. Sourer. "Kinetics and Thermal Characterization of Thermoset Cure." *Polymer Engineering and Science*, vol. 13, pp. 59-74, 1973.

| <u>NO. OF COPIES</u> | <u>ORGANIZATION</u> |
|--------------------------|---|
| 2 | DEFENSE TECHNICAL INFORMATION CENTER DTIC DDA 8725 JOHN J KINGMAN RD STE 0944 FT BELVOIR VA 22060-6218 |
| 1 | HQDA DAMO FDQ D SCHMIDT 400 ARMY PENTAGON WASHINGTON DC 20310-0460 |
| 1 | OSD OUSD(A&T)/ODDDR&E(R) R J TREW THE PENTAGON WASHINGTON DC 20301-7100 |
| 1 | DPTY CG FOR RDA US ARMY MATERIEL CMD AMCRDA 5001 EISENHOWER AVE ALEXANDRIA VA 22333-0001 |
| 1 | INST FOR ADVNCD TCHNLGY THE UNIV OF TEXAS AT AUSTIN PO BOX 202797 AUSTIN TX 78720-2797 |
| 1 | DARPA B KASPAR 3701 N FAIRFAX DR ARLINGTON VA 22203-1714 |
| 1 | NAVAL SURFACE WARFARE CTR CODE B07 J PENNELLA 17320 DAHLGREN RD BLDG 1470 RM 1101 DAHLGREN VA 22448-5100 |
| 1 | US MILITARY ACADEMY MATH SCI CTR OF EXCELLENCE DEPT OF MATHEMATICAL SCI MADN MATH THAYER HALL WEST POINT NY 10996-1786 |

| <u>NO. OF COPIES</u> | <u>ORGANIZATION</u> |
|--------------------------|--|
| 1 | DIRECTOR US ARMY RESEARCH LAB AMSRL DD J J ROCCHIO 2800 POWDER MILL RD ADELPHI MD 20783-1197 |
| 1 | DIRECTOR US ARMY RESEARCH LAB AMSRL CS AS (RECORDS MGMT) 2800 POWDER MILL RD ADELPHI MD 20783-1145 |
| 3 | DIRECTOR US ARMY RESEARCH LAB AMSRL CI LL 2800 POWDER MILL RD ADELPHI MD 20783-1145 |
| | <u>ABERDEEN PROVING GROUND</u> |
| 4 | DIR USARL AMSRL CI LP (BLDG 305) |

| <u>NO. OF COPIES</u> | <u>ORGANIZATION</u> | <u>NO OF. COPIES</u> | <u>ORGANIZATION</u> |
|--------------------------|---|--------------------------|--|
| 1 | DIRECTOR USARL AMSRL CP CA D SNIDER 2800 POWDER MILL RD ADELPHI MD 20783 | 5 | COMMANDER USA ARDEC AMSTA AR CCH S MUSALLI R CARR M LUCIANO T LOUCEIRO PICATINNY ARSENAL NJ 07806-5000 |
| 1 | COMMANDER USA ARDEC AMSTA AR FSE T GORA PICATINNY ARSENAL NJ 07806-5000 | 4 | COMMANDER USA ARDEC AMSTA AR (2CPS) E FENNEL (2 CPS) PICATINNY ARSENAL NJ 07806-5000 |
| 3 | COMMANDER USA ARDEC AMSTA AR TD PICATINNY ARSENAL NJ 078806-5000 | 1 | COMMANDER USA ARDEC AMSTA AR CCH P J LUTZ PICATINNY ARSENAL NJ 07806-5000 |
| 5 | COMMANDER USA TACOM AMSTA JSK S GOODMAN J FLORENCE AMSTA TR D B RAJU L HINOJOSA D OSTBERG WARREN MI 48397-5000 | 1 | COMMANDER USA ARDEC AMSTA AR FSF T C LIVECCHIA PICATINNY ARSENAL NJ 07806-5000 |
| 5 | PM SADARM SFAE GCSS SD COL B ELLIS M DEVINE W DEMASSI J PRITCHARD S HROWNAK PICATINNY ARSENAL NJ 07806-5000 | 1 | COMMANDER USA ARDEC AMSTA AR QAC T/C C PATEL PICATINNY ARSENAL NJ 07806-5000 |
| 1 | COMMANDER USA ARDEC F MCLAUGHLIN PICATINNY ARSENAL NJ 07806-5000 | 2 | COMMANDER USA ARDEC AMSTA AR M D DEMELLA F DIORIO PICATINNY ARSENAL NJ 07806-5000 |

NO. OF
COPIES ORGANIZATION

3 COMMANDER
USA ARDEC
AMSTA AR FSA
A WARNASH
B MACHAK
M CHIEFA
PICATINNY ARSENAL NJ
07806-5000

1 COMMANDER
SMCWV QAE Q
B VANINA
BLDG 44 WATERVLIET ARSENAL
WATERVLIET NY 12189-4050

1 COMMANDER
SMCWV SPM
T MCCLOSKEY
BLDG 253 WATERVLIET ARSENAL
WATERVLIET NY 12189-4050

8 DIRECTOR
BENET LABORATORIES
AMSTA AR CCB
J KEANE
J BATTAGLIA
J VASILAKIS
G FFIAR
V MONTVORI
G DANDREA
R HASENBEIN
AMSTA AR CCB R
S SOPOK
WATERVLIET NY 12189-4050

1 COMMANDER
SMCWV QA QS K INSCO
WATERVLIET NY 12189-4050

1 COMMANDER
PRODUCTION BASE MODERN
ACTY
USA ARDEC
AMSMC PBM K
PICATINNY ARSENAL NJ
07806-5000

NO OF.
COPIES ORGANIZATION

1 COMMANDER
USA BELVOIR RD&E CTR
STRBE JBC
FT BELVOIR VA 22060-5606

2 COMMANDER
USA ARDEC
AMSTA AR FSB G
M SCHIKSNIS
D CARLUCCI
PICATINNY ARSENAL NJ
07806-5000

1 US ARMY COLD REGIONS
RESEARCH & ENGINEERING CTR
P DUTTA
72 LYME RD
HANVOVER NH 03755

1 DIRECTOR
USARL
AMSRL WT L D WOODBURY
2800 POWDER MILL RD
ADELPHI MD 20783-1145

1 COMMANDER
USA MICOM
AMSMI RD W MCCORKLE
REDSTONE ARSENAL AL
35898-5247

1 COMMANDER
USA MICOM
AMSMI RD ST P DOYLE
REDSTONE ARSENAL AL
35898-5247

1 COMMANDER
USA MICOM
AMSMI RD ST CN T VANDIVER
REDSTONE ARSENAL AL
35898-5247

3 US ARMY RESEARCH OFFICE
A CROWSON
K LOGAN
J CHANDRA
PO BOX 12211
RESEARCH TRIANGLE PARK NC
27709-2211

| <u>NO. OF COPIES</u> | <u>ORGANIZATION</u> |
|----------------------|---|
| 3 | US ARMY RESEARCH OFFICE ENGINEERING SCIENCES DIV R SINGLETON G ANDERSON K IYER PO BOX 12211 RESEARCH TRIANGLE PARK NC 27709-2211 |
| 5 | PM TMAS SFAE GSSC TMA COL PAWLICKI K KIMKER E KOPACZ R ROESER B DORCY PICATINNY ARSENAL NJ 07806-5000 |
| 1 | PM TMAS SFAE GSSC TMA SMD R KOWALSKI PICATINNY ARSENAL NJ 07806-5000 |
| 3 | PEO FIELD ARTILLERY SYSTEMS SFAE FAS PM H GOLDMAN T MCWILLIAMS T LINDSAY PICATINNY ARSENAL NJ 07806-5000 |
| 2 | PM CRUSADER G DELCOCO J SHIELDS PICATINNY ARSENAL NJ 07806-5000 |
| 3 | NASA LANGLEY RESEARCH CTR MS 266 AMSRL VS W ELBER F BARTLETT JR C DAVILA HAMPTON VA 23681-0001 |

| <u>NO OF. COPIES</u> | <u>ORGANIZATION</u> |
|----------------------|---|
| 2 | COMMANDER DARPA S WAX 2701 N FAIRFAX DR ARLINGTON VA 22203-1714 |
| 6 | COMMANDER WRIGHT PATTERSON AFB WL FIV A MAYER WL MLBM S DONALDSON T BENSON-TOLLE C BROWNING J MCCOY F ABRAMS 2941 P ST STE 1 DAYTON OH 45433 |
| 2 | NAVAL SURFACE WARFARE CTR DAHLGREN DIV CODE G06 R HUBBARD CODE G 33 C DAHLGREN VA 22448 |
| 1 | NAVAL RESEARCH LAB I WOLOCK CODE 6383 WASHINGTON DC 20375-5000 |
| 1 | OFFICE OF NAVAL RESEARCH MECH DIV Y RAJAPAKSE CODE 1132SM ARLINGTON VA 22271 |
| 1 | NAVAL SURFACE WARFARE CTR CRANE DIV M JOHNSON CODE 20H4 LOUISVILLE KY 40214-5245 |
| 1 | DAVID TAYLOR RESEARCH CTR SHIP STRUCTURES & PROTECTION DEPT J CORRADO CODE 1702 BETHESDA MD 20084 |
| 2 | DAVID TAYLOR RESEARCH CTR R ROCKWELL W PHYLLAIER BETHESDA MD 20054-5000 |

| <u>NO. OF COPIES</u> | <u>ORGANIZATION</u> | <u>NO OF. COPIES</u> | <u>ORGANIZATION</u> |
|----------------------|---|----------------------|--|
| 1 | DEFENSE NUCLEAR AGENCY INNOVATIVE CONCEPTS DIV R ROHR 6801 TELEGRAPH RD ALEXANDRIA VA 22310-3398 | 2 | DIRECTOR LLNL F ADDESSIO MS B216 J REPPA MS F668 PO BOX 1633 LOS ALAMOS NM 87545 |
| 1 | EXPEDITIONARY WARFARE DIV N85 F SHOUP 2000 NAVY PENTAGON WASHINGTON DC 20350-2000 | 3 | UNITED DEFENSE LP 4800 EAST RIVER DR P JANKE MS170 T GIOVANETTI MS236 B VAN WYK MS 389 MINNEAPOLIS MN 55421-1498 |
| 1 | OFFICE OF NAVAL RESEARCH D SIEGEL 351 800 N QUINCY ST ARLINGTON VA 22217-5660 | 4 | DIRECTOR SANDIA NATIONAL LAB APPLIED MECHANICS DEPT DIV 8241 W KAWAHARA K PERANO D DAWSON P NIELAN PO BOX 969 LIVERMORE CA 94550-0096 |
| 7 | NAVAL SURFACE WARFARE CTR J H FRANCIS CODE G30 D WILSON CODE G32 R D COOPER CODE G32 E ROWE CODE G33 T DURAN CODE G33 L DE SIMONE CODE G33 DAHLGREN VA 22448 | 1 | BATTALLE C R HARGREAVES 505 KNIG AVE COLUMBUS OH 43201-2681 |
| 1 | COMMANDER NAVAL SEA SYSTEM CMD P LIESE 2351 JEFFERSON DAVIS HIGHWAY ARLINGTON VA 22242-5160 | 1 | PACIFIC NORTHWEST LAB M SMITH PO BOX 999 RICHLAND WA 99352 |
| 1 | NAVAL SURFACE WARFARE CTR M E LACY CODE B02 17320 DAHLGREN RD DAHLGREN VA 22448 | 1 | LLNL M MURPHY PO BOX 808 L 282 LIVERMORE CA 94550 |
| 1 | NAVAL WARFARE SURFACE CTR TECH LIBRARY CODE 323 17320 DAHLGREN RD DAHLGREN VA 22448 | 10 | UNIV OF DELAWARE CTR FOR OCMPOSITE MATERIALS J GILLESPIE 201 SPENCER LAB NEWARK DE 19716 |
| 4 | DIR LLNL R CHRISTENSEN S DETERESA F MAGMESS M FINGER PO BOX 808 LIVERMORE CA 94550 | | |

| <u>NO. OF COPIES</u> | <u>ORGANIZATION</u> | <u>NO OF. COPIES</u> | <u>ORGANIZATION</u> |
|----------------------|---|----------------------|---|
| 2 | THE U OF TEXAS AT AUSTIN CTR ELECTROMECHANICS A WALLIS J KITZMILLER 10100 BURNET RD AUSTIN TX 78758-4497 | 1 | NOESIS INC 1110 N GLEBE RD STE 250 ARLINGTON VA 22201-4795 |
| 1 | AAI CORPORATION T G STASTNY PO BOX 126 HUNT VALLEY MD 21030-0126 | 1 | ARROW TECH ASSO 1233 SHELBURNE RD STE D 8 SOUTH BURLINGTON VT 05403-7700 |
| 1 | SAIC D DAKIN 2200 POWELL ST STE 1090 EMERYVILLE CA 94608 | 5 | GEN CORP AEROJET D PILLASCH T COULTER C FLYNN D RUBAREZUL M GREINER 1100 WEST HOLLYVALE ST AZUSA CA 91702-0296 |
| 1 | SAIC M PALMER 2109 AIR PARK RD S E ALBUQUERQUE NM 87106 | 1 | NIST STRUCTURE & MECHANICS GRP POLYMER DIV POLYMERS RM A209 G MCKENNA GAITHERSBURG MD 20899 |
| 1 | SAIC R ACEBAL 1225 JOHNSON FERRY RD STE 100 MARIETTA GA 30068 | 1 | GENERAL DYNAMICS LAND SYSTEM DIVISION D BARTLE PO BOX 1901 WARREN MI 48090 |
| 1 | SAIC G CHRYSSOMALLIS 3800 W 80TH ST STE 1090 BLOOMINGTON MN 55431 | 4 | INSTITUTE FOR ADVANCED TECHNOLOGY H FAIR P SULILVAN W REINECKE I MCNAB 4030 2 W BRAKER LN AUSTIN TX 78759 |
| 6 | ALLIANT TECHSYSTEMS INC C CANDLAND R BECKER L LEE R LONG D KAMDAR G KASSUELKE 600 2ND ST NE HOPKINS MN 55343-8367 | 1 | PM ADVANCED CONCEPTS LORAL VOUGHT SYSTEMS J TAYLOR MS WT 21 PO BOX 650003 DALLAS TX 76265-0003 |
| 1 | CUSTOM ANALYTICAL ENGR SYS INC A ALEXANDER 13000 TENSOR LANE NE FLINTSTONE MD 21530 | | |

| <u>NO. OF COPIES</u> | <u>ORGANIZATION</u> | <u>NO OF. COPIES</u> | <u>ORGANIZATION</u> |
|--------------------------|--|--------------------------|---|
| 2 | UNITED DEFENSE LP P PARA G THOMASA 1107 COLEMAN AVE BOX 367 SAN JOSE CA 95103 | 4 | NIST POLYMERS DIVISION R PARNAS J DUNKERS M VANLANDINGHAM D HUNSTON GAITHERSBURG MD 20899 |
| 1 | MARINE CORPS SYSTEMS CMD PM GROUND WPNS COL R OWEN 2083 BARNETT AVE STE 315 QUANTICO VA 22134-5000 | 1 | OAK RIDGE NATIONAL LAB A WERESZCZAK BLDG 4515 MS 6069 PO BOX 2008 OAKRIDGE TN 37831-6064 |
| 1 | OFFICE OF NAVAL RES J KELLY 800 NORTH QUINCEY ST ARLINGTON VA 22217-5000 | 1 | COMMANDER USA ARDEC INDUSTRIAL ECOLOGY CTR T SACHAR BLDG 172 PICATINNY ARSENAL NJ 07806-5000 |
| 1 | NAVSEE OJRI G CAMPONESCHI 2351 JEFFERSON DAVIS HWY ARLINGTON VA 22242-5160 | 1 | COMMANDER USA ATCOM AVIATION APPLIED TECH DIR J SCHUCK FT EUSTIS VA 23604 |
| 1 | USAF WL MLS O L A HAKIM 5525 BAILEY LOOP 243E MCCLELLAN AFB CA 55552 | 1 | COMMANDER USA ARDEC AMSTA AR SRE D YEE PICATINNY ARSENAL NJ 07806-5000 |
| 1 | NASA LANGLEY J MASTERS MS 389 HAMPTON VA 23662-5225 | 1 | COMMANDER USA ARDEC AMSTA AR QAC T D RIGOGLIOSO BLDG 354 M829E3 IPT PICATINNY ARSENAL NJ 07806-5000 |
| 2 | FAA TECH CTR D OPLINGER AAR 431 P SHYPRYKEVICH AAR 431 ATLANTIC CITY NJ 08405 | 1 | COMMANDER USA ARDEC AMSTA AR QAC T D RIGOGLIOSO BLDG 354 M829E3 IPT PICATINNY ARSENAL NJ 07806-5000 |
| 1 | NASA LANGLEY RC CC POE MS 188E NEWPORT NEWS VA 23608 | | |
| 1 | USAF WL MLBC E SHINN 2941 PST STE 1 WRIGHT PATTERSON AFB OH 45433-7750 | | |

NO. OF
COPIES ORGANIZATION

7 COMMANDER
USA ARDEC
AMSTA AR CCH B
B KONRAD
E RIVERA
G EUSTICE
S PATEL
G WAGNECZ
R SAYER
F CHANG
BLDG 65
PICATINNY ARSENAL NJ
07806-5000

6 DIRECTOR
US ARMY RESEARCH LAB
AMSRL WM MB
A ABRAHAMIAN
M BERMAN
A FRYDMAN
T LI
W MCINTOSH
E SZYMANSKI
2800 POWDER MILL RD
ADELPHI MD 20783-1197

ABERDEEN PROVING GROUND

67 DIR USARL
AMSRL CI
AMSRL CI C
W STUREK
AMSRL CI CB
R KASTE
AMSRL CI S
A MARK
AMSRL SL B
AMSRL SL BA
AMSRL SL BE
D BELY
AMSRL WM B
A HORST
E SCHMIDT
AMSRL WM BE
G WREN
C LEVERITT
D KOOKER

NO OF.
COPIES ORGANIZATION

AMSRL WM BC
P PLOSTINS
D LYON
J NEWILL
AMSRL WM BD
S WILKERSON
R FIFER
B FORCH
R PESCE RODRIGUEZ
B RICE
AMSRL WM
D VIECHNICKI
G HAGNAUER
J MCCAULEY
AMSRL WM MA
R SHUFORD
S MCKNIGHT
L GHIORSE
AMSRL WM MB
V HARIK
J SANDS
W DRYSDALE
J BENDER
T BLANAS
T BOGETTI
R BOSSOLI
L BURTON
S CORNELISON
P DEHMER
R DOOLEY
B FINK
G GAZONAS
S GHIORSE
D GRANVILLE
D HOPKINS
C HOPPEL
D HENRY
R KASTE
M LEADORE
R LIEB
E RIGAS
D SPAGNUOLO
W SPURGEON
J TZENG
AMSRL WM MC
J BEATTY
AMSRL WM MD
W ROY
AMSRL WM T
B BURNS

NO. OF
COPIES ORGANIZATION

ABERDEEN PROVING GROUND (CONT)

AMSRL WM TA
 W GILLICH
 E RAPACKI
 T HAVEL
AMSRL WM TC
 R COATES
 W DE ROSSET
AMSRL WM TD
 W BRUCHEY
 A D GUPTA
AMSRL WM BB
 H ROGERS
AMSRL WM BA
 F BRANDON
 W D AMICO
AMSRL WM BR
 J BORNSTEIN
AMSRL WM TE
 A NILER
AMSRL WM BF
 J LACETERA

INTENTIONALLY LEFT BLANK.

| REPORT DOCUMENTATION PAGE | | | Form Approved OMB No. 0704-0188 | |
|--|--|--|---|--|
| Public reporting burden for this collection of information is estimated to average 1 hour per response, including the time for reviewing instructions, searching existing data sources, gathering and maintaining the data needed, and completing and reviewing the collection of information. Send comments regarding this burden estimate or any other aspect of this collection of information, including suggestions for reducing this burden, to Washington Headquarters Services, Directorate for Information Operations and Reports, 1215 Jefferson Davis Highway, Suite 1204, Arlington, VA 22202-4302, and to the Office of Management and Budget, Paperwork Reduction Project (0704-0188), Washington, DC 20503. | | | | |
| 1. AGENCY USE ONLY (Leave blank) | 2. REPORT DATE November 1999 | 3. REPORT TYPE AND DATES COVERED Final, Jan 98 - Sep 98 | | |
| 4. TITLE AND SUBTITLE Non-Polluting Composites Repair and Remanufacturing for Military Applications: Induction-Based Repair of Integral Armor | | | 5. FUNDING NUMBERS AH42 | |
| 6. AUTHOR(S) Bruce K. Fink, Steven H. McKnight, Shridhar Yarlagadda,* and John W. Gillespie Jr.* | | | | |
| 7. PERFORMING ORGANIZATION NAME(S) AND ADDRESS(ES) U.S. Army Research Laboratory ATTN: AMSRL-WM-MB Aberdeen Proving Ground, MD 21005-5069 | | | 8. PERFORMING ORGANIZATION REPORT NUMBER ARL-TR-2121 | |
| 9. SPONSORING/MONITORING AGENCY NAME(S) AND ADDRESS(ES) | | | 10. SPONSORING/MONITORING AGENCY REPORT NUMBER | |
| 11. SUPPLEMENTARY NOTES *University of Delaware, Newark, DE 19716 | | | | |
| 12a. DISTRIBUTION/AVAILABILITY STATEMENT Approved for public release; distribution is unlimited. | | | 12b. DISTRIBUTION CODE | |
| 13. ABSTRACT (Maximum 200 words) Polymer-matrix composite material and structural adhesive repair and manufacturing have significant environmental costs. These costs have recently been documented based on current and anticipated future Department of Defense (DOD) use of these materials. The principal issues for reducing the environmental impact and its associated cost are (1) reduction in hazardous waste by eliminating shelf-life limitations, (2) reduction in nitrogen oxides (NO _x) by replacing global heating of the part with localized heating, (3) reduction in volatile organic compound (VOC) emissions by accelerated curing and containment, and (4) reduction in hazardous waste by minimizing production debris through processing step management. Induction-based adhesive curing is a potential replacement for current repair and manufacturing methods to resolve the principal issues. The current work establishes that induction heating using conductive mesh susceptors can be used to rapidly cure thermosetting adhesives under a VOC-reducing vacuum condition. It is also established that the presence of these susceptor materials, although not optimized, does not adversely affect the mechanical performance of the bondline when considering the low scatter in lap shear strength. The feasibility of induction-based repair using metallic screen susceptors and the applicability of induction heating to multilayer single-step bonding wherein heat generation is limited to localized bondline regions allowing optimization of repair processes are demonstrated. | | | | |
| 14. SUBJECT TERMS co-injection resin transfer molding, flow modeling, composite material | | | 15. NUMBER OF PAGES 46 | |
| | | | 16. PRICE CODE | |
| 17. SECURITY CLASSIFICATION OF REPORT UNCLASSIFIED | 18. SECURITY CLASSIFICATION OF THIS PAGE UNCLASSIFIED | 19. SECURITY CLASSIFICATION OF ABSTRACT UNCLASSIFIED | 20. LIMITATION OF ABSTRACT SAR | |

INTENTIONALLY LEFT BLANK.

USER EVALUATION SHEET/CHANGE OF ADDRESS

This Laboratory undertakes a continuing effort to improve the quality of the reports it publishes. Your comments/answers to the items/questions below will aid us in our efforts.

1. ARL Report Number/Author ARL-TR-2121 (Fink) Date of Report October 1999

2. Date Report Received _____

3. Does this report satisfy a need? (Comment on purpose, related project, or other area of interest for which the report will be used.) _____

4. Specifically, how is the report being used? (Information source, design data, procedure, source of ideas, etc.) _____

5. Has the information in this report led to any quantitative savings as far as man-hours or dollars saved, operating costs avoided, or efficiencies achieved, etc? If so, please elaborate. _____

6. General Comments. What do you think should be changed to improve future reports? (Indicate changes to organization, technical content, format, etc.) _____

CURRENT
ADDRESS

Organization

Name

E-mail Name

Street or P.O. Box No.

City, State, Zip Code

7. If indicating a Change of Address or Address Correction, please provide the Current or Correct address above and the Old or Incorrect address below.

OLD
ADDRESS

Organization

Name

Street or P.O. Box No.

City, State, Zip Code

(Remove this sheet, fold as indicated, tape closed, and mail.)
(DO NOT STAPLE)